

Supporting Information

Rb₃In(SO₄)₃: a Defluorinated Mixed Main-Group Metal Sulfate for Ultraviolet Transparent Nonlinear Optical Material with Large Optical Band Gap

Qinke Xu,^{a,δ} Xingxing Jiang,^{b,δ} Chao Wu,^{a,δ} Lin Lin,^a Zhipeng Huang,^a Zheshuai Lin,^b Mark G. Humphrey,^c and Chi Zhang*,^a

^a China-Australia Joint Research Center for Functional Molecular Materials, School of Chemical Science and Engineering, Tongji University, Shanghai 200092, China

^b Key Lab of Functional Crystals and Laser Technology, Technical Institute of Physics and Chemistry, Chinese Academy of Sciences, Beijing 100190, China

^c Research School of Chemistry, Australian National University, Canberra, Australian Capital Territory 2601, Australia

^δ These authors contributed equally to this work

CONTENTS

Theoretical Calculations

Table S1. Selected bond distances (\AA) and angles ($^{\circ}$) for $\text{Rb}_2\text{InF}_3(\text{SO}_4)$ and $\text{Rb}_3\text{In}(\text{SO}_4)_3$.

Table S2. Atomic coordinates ($\times 10^4$), equivalent isotropic displacement parameters ($\text{\AA}^2 \times 10^3$), and the bond valence sum for each atom in the asymmetric unit of $\text{Rb}_2\text{InF}_3(\text{SO}_4)$.

Table S3. Atomic coordinates ($\times 10^4$), equivalent isotropic displacement parameters ($\text{\AA}^2 \times 10^3$), and the bond valence sum for each atom in the asymmetric unit of $\text{Rb}_3\text{In}(\text{SO}_4)_3$.

Figure S1. Photograph of crystals of (a) $\text{Rb}_2\text{InF}_3(\text{SO}_4)$ and (b) $\text{Rb}_3\text{In}(\text{SO}_4)_3$.

Figure S2. Energy dispersive spectroscopy results of (a) $\text{Rb}_2\text{InF}_3(\text{SO}_4)$ and (b) $\text{Rb}_3\text{In}(\text{SO}_4)_3$.

Figure S3. The asymmetric unit of (a) $\text{Rb}_2\text{InF}_3(\text{SO}_4)$ and (b) $\text{Rb}_2\text{InF}_3(\text{SO}_4)$.

Figure S4. Powder X-ray diffraction patterns of (a) $\text{Rb}_2\text{InF}_3(\text{SO}_4)$ and (b) $\text{Rb}_3\text{In}(\text{SO}_4)_3$.

Figure S5. Infrared spectra of (a) $\text{Rb}_2\text{InF}_3(\text{SO}_4)$ and (b) $\text{Rb}_3\text{In}(\text{SO}_4)_3$.

Figure S6. Thermogravimetric analyses of (a) $\text{Rb}_2\text{InF}_3(\text{SO}_4)$ and (b) $\text{Rb}_3\text{In}(\text{SO}_4)_3$ under a N_2 atmosphere.

Figure S7. Calculated band structures of $\text{Rb}_3\text{In}(\text{SO}_4)_3$.

Figure S8. Calculated refractive indexes of $\text{Rb}_3\text{In}(\text{SO}_4)_3$.

References

Theoretical Calculations:

First-principles calculations on $\text{Rb}_3\text{In}(\text{SO}_4)_3$ were performed using the CASTEP package,¹ a total energy package based on pseudopotential density functional theory (DFT).² The correlation-exchange terms in the Hamiltonian were described by the functional developed by Perdew, Burke, and Ernzerhof³ in the generalized gradient approximation form. Optimized norm-conserving pseudopotentials in the Kleinman–Bylander⁴ form were adopted to model the effective interaction between the valence electrons and atom cores, which allows the choice of a relatively small plane-wave basis set without compromising the computational accuracy. A kinetic energy cutoff of 850 eV and dense Monkhorst-Pack⁵ k -point meshes spanning less than 0.03 Å³ in the Brillouin zone were chosen.

Because of the discontinuity of exchange-correlation in the framework of standard DFT, the calculated band gaps are usually smaller than the experimental values, and so a scissor operator⁶ was used to shift the conduction bands (CB) to match the values. Based on the scissor-corrected electron band structure, the imaginary part of the dielectric constants can be calculated by the electron transition from the valence bands (VB) to the CB. Accordingly, the real part of the dielectric constant, the refractive index, can be determined by a Kramers–Kronig transform of the calculated imaginary part.⁷ The refractive indices n and the birefringence Δn were thereby obtained. The anisotropic SHG coefficient tensor was calculated from a formula based on gauge formalism developed by our group.^{8–9} To gain insight into the contribution of the constituent groups to the SHG coefficient, an SHG-weighted electron density analysis were performed. In the SHG-weighted electron density analysis, the electron density of all the orbitals is summed by a weight positively correlated with its contribution to the SHG coefficient, and thus the electronic cloud of orbitals crucial to the SHG response is highlighted in real space.¹⁰

Table S1. Selected bond distances (\AA) and angles (deg.) for $\text{Rb}_2\text{InF}_3(\text{SO}_4)$ and $\text{Rb}_3\text{In}(\text{SO}_4)_3^{\text{a}}$.

$\text{Rb}_2\text{InF}_3(\text{SO}_4)$			
In(3)-F(2)	2.022(6)	In(3)-F(6)#1	2.118(4)
In(3)-F(2)#1	2.022(6)	In(3)-O(12)#1	2.130(7)
In(3)-F(6)	2.118(4)	In(3)-O(12)	2.130(7)
S(1)-O(5)	1.442(9)	S(1)-O(12)	1.500(7)
S(1)-O(5)#6	1.442(9)	S(1)-O(12)#6	1.500(7)
Rb(1)-F(2)#10	2.840(6)	Rb(1)-F(6)#12	3.008(6)
Rb(1)-O(5)#11	2.845(9)	Rb(1)-O(5)#13	3.013(9)
Rb(1)-F(2)#8	2.972(6)	Rb(1)-O(5)#6	3.390(9)
F(2)-In(3)-F(2)#1	180	F(6)-In(3)-O(12)#1	87.6(3)
F(2)-In(3)-F(6)	87.99(18)	F(6)#1-In(3)-O(12)#1	92.4(3)
F(2)#1-In(3)-F(6)	92.01(18)	F(2)-In(3)-O(12)	86.6(3)
F(2)-In(3)-F(6)#1	92.01(18)	F(2)#1-In(3)-O(12)	93.4(3)
F(2)#1-In(3)-F(6)#1	87.99(18)	F(6)-In(3)-O(12)	92.4(3)
F(6)-In(3)-F(6)#1	180.000(1)	F(6)#1-In(3)-O(12)	87.6(3)
F(2)-In(3)-O(12)#1	93.4(3)	O(12)#1-In(3)-O(12)	180.0(4)
F(2)#1-In(3)-O(12)#1	86.6(3)		
O(5)-S(1)-O(5)#6	114.1(7)	O(5)-S(1)-O(12)#6	107.5(4)
O(5)-S(1)-O(12)	109.9(4)	O(5)#6-S(1)-O(12)#6	109.9(4)
O(5)#6-S(1)-O(12)	107.5(4)	O(12)-S(1)-O(12)#6	107.7(6)
$\text{Rb}_3\text{In}(\text{SO}_4)_3$			
In(1)-O(3)#1	2.128(5)	In(1)-O(1)#4	2.137(4)
In(1)-O(3)#2	2.128(5)	In(1)-O(1)#5	2.137(4)
In(1)-O(3)#3	2.128(5)	In(1)-O(1)	2.137(4)
S(3)-O(4)	1.424(4)	S(3)-O(3)	1.455(4)
S(3)-O(2)	1.440(4)	S(3)-O(1)	1.475(4)
Rb(2)-O(4)#12	2.793(5)	Rb(2)-O(2)#16	3.331(6)
Rb(2)-O(2)#13	2.907(4)	Rb(2)-O(4)#16	3.442(9)
Rb(2)-O(1)#14	2.914(4)	Rb(2)-O(2)#15	3.511(7)
Rb(2)-O(2)#14	3.190(6)	Rb(2)-S(3)#14	3.5783(10)
Rb(2)-O(3)#15	3.221(5)	Rb(2)-S(3)#16	3.7210(11)
O(3)#1-In(1)-O(3)#2	98.49(18)	O(3)#3-In(1)-O(1)#5	89.7(2)
O(3)#1-In(1)-O(3)#3	98.49(18)	O(1)#4-In(1)-O(1)#5	91.72(17)
O(3)#2-In(1)-O(3)#3	98.49(18)	O(3)#1-In(1)-O(1)	89.7(2)
O(3)#1-In(1)-O(1)#4	171.8(2)	O(3)#2-In(1)-O(1)	80.14(18)
O(3)#2-In(1)-O(1)#4	89.7(2)	O(3)#3-In(1)-O(1)	171.8(2)
O(3)#3-In(1)-O(1)#4	80.14(18)	O(1)#4-In(1)-O(1)	91.72(17)
O(3)#1-In(1)-O(1)#5	80.14(18)	O(1)#5-In(1)-O(1)	91.72(17)
O(3)#2-In(1)-O(1)#5	171.8(2)		
O(4)-S(3)-O(2)	112.3(4)	O(4)-S(3)-O(1)	110.5(3)
O(4)-S(3)-O(3)	112.2(5)	O(2)-S(3)-O(1)	107.6(3)
O(2)-S(3)-O(3)	106.2(3)	O(3)-S(3)-O(1)	107.8(3)

^a Symmetry codes:

Rb₂InF₃(SO₄): #1 -x, -y+1, -z+1; #2 -x+1/2, y+1/2, z; #3 x-1/2, -y+1/2, -z+1; #4 x-1/2, y+1/2, -z+1/2; #5 -x+1/2, -y+1/2, z+1/2; #6 -x, y, -z+1/2; #7 x-1/2, y-1/2, -z+1/2; #8 -x+1/2, y-1/2, z; #9 x, -y+1, z+1/2; #10 x, -y+1, z-1/2; #11 x+1/2, y+1/2, -z+1/2; #12 x+1/2, y-1/2, -z+1/2; #13 x+1/2, -y+1/2, -z+1.

Rb₃In(SO₄)₃: #1 -x+y, y, z+1/2; #2 x, x-y, z+1/2; #3 -y, -x, z+1/2; #4 -x+y, -x, z; #5 -y, x-y, z; #6 -y+2/3, x-y+1/3, z+1/3; #7 x-1/3, y-2/3, z+1/3; #8 -x+y-1/3, -x+1/3, z+1/3; #9 x+1/3, x-y+2/3, z+1/6; #10 -y+2/3, -x+1/3, z-1/6; #11 -y, -x, z-1/2; #12 -y+1/3, x-y+2/3, z-1/3; #13 x-1/3, x-y+1/3, z-1/6; #14 -x+y+1/3, -x+2/3, z-1/3; #15 -y+1/3, -x+2/3, z+1/6; #16 -x+y, y, z-1/2.

Table S2. Atomic coordinates ($\times 10^4$), equivalent isotropic displacement parameters ($\text{\AA}^2 \times 10^3$), and the bond valence sum for each atom in the asymmetric unit of $\text{Rb}_2\text{InF}_3(\text{SO}_4)$. $U(\text{eq})$ is defined as one third of the trace of the orthogonalized U_{ij} tensor.

Atom	Wyck	X	Y	Z	U_{eq} (\AA^2)	BVS
In(1)	4b	0	5000	5000	13(1)	2.97
S(1)	4c	0	1912(4)	2500	18(1)	6.05
O(1)	8d	-905(8)	1024(10)	3316(12)	24(1)	2.09
O(2)	8d	559(6)	2914(8)	3863(10)	22(2)	1.97
F(1)	8d	1702(5)	5533(7)	5219(8)	36(2)	1.03
F(2)	4c	0	6105(10)	2500	23(2)	0.92
Rb(1)	8d	3067(1)	3345(1)	3074(1)	26(1)	0.97

Table S3. Atomic coordinates ($\times 10^4$), equivalent isotropic displacement parameters ($\text{\AA}^2 \times 10^3$), and the bond valence sum for each atom in the asymmetric unit of $\text{Rb}_3\text{In}(\text{SO}_4)_3$. $U(\text{eq})$ is defined as one third of the trace of the orthogonalized U_{ij} tensor.

Atom	Wyck	X	Y	Z	U_{eq} (\AA^2)	BVS
In(1)	6a	0	0	5073(1)	23(1)	3.22
S(1)	18b	1441(1)	1762(1)	2575(1)	19(1)	6.43
O(1)	18b	1233(3)	1038(3)	3766(4)	45(1)	2.19
O(2)	18b	2504(3)	2444(3)	2549(8)	65(1)	1.96
O(3)	18b	1196(4)	1216(5)	1199(5)	72(2)	2.13
O(4)	18b	887(5)	2264(4)	2783(8)	88(2)	2.21
Rb(1)	18b	1161(1)	3650(1)	559(1)	35(1)	1.05

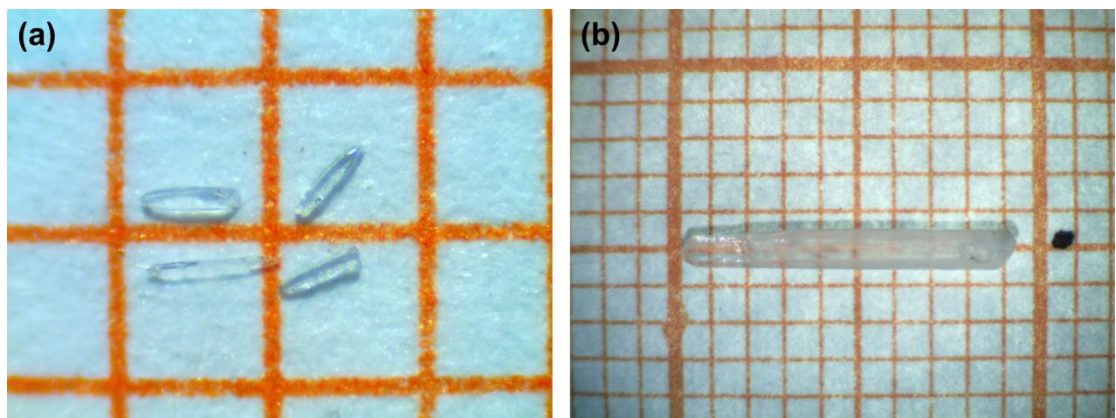


Figure S1. Photograph of crystals of (a) $\text{Rb}_2\text{InF}_3(\text{SO}_4)$ and (b) $\text{Rb}_3\text{In}(\text{SO}_4)_3$.

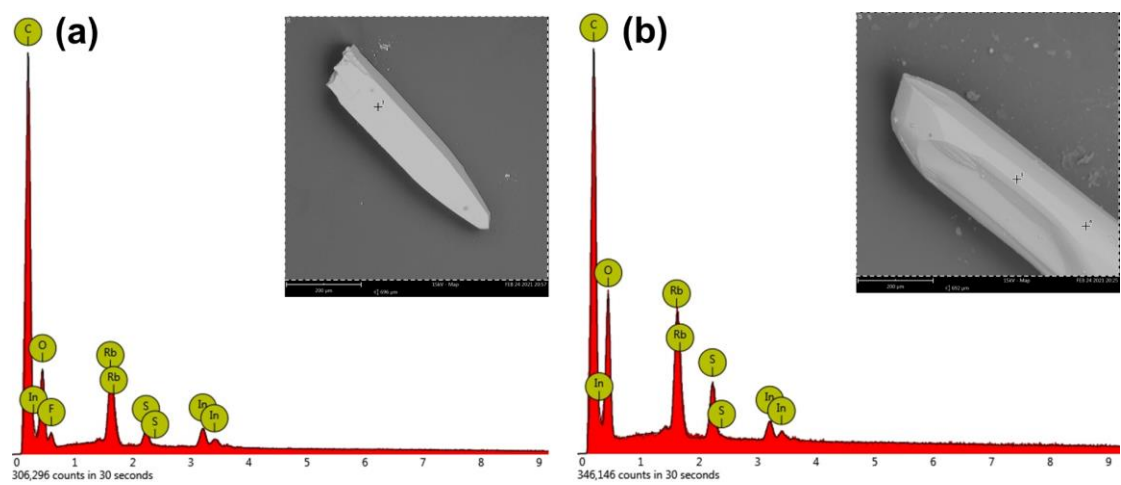


Figure S2. Energy dispersive spectroscopy results of (a) $\text{Rb}_2\text{InF}_3(\text{SO}_4)$ and (b) $\text{Rb}_3\text{In}(\text{SO}_4)_3$.

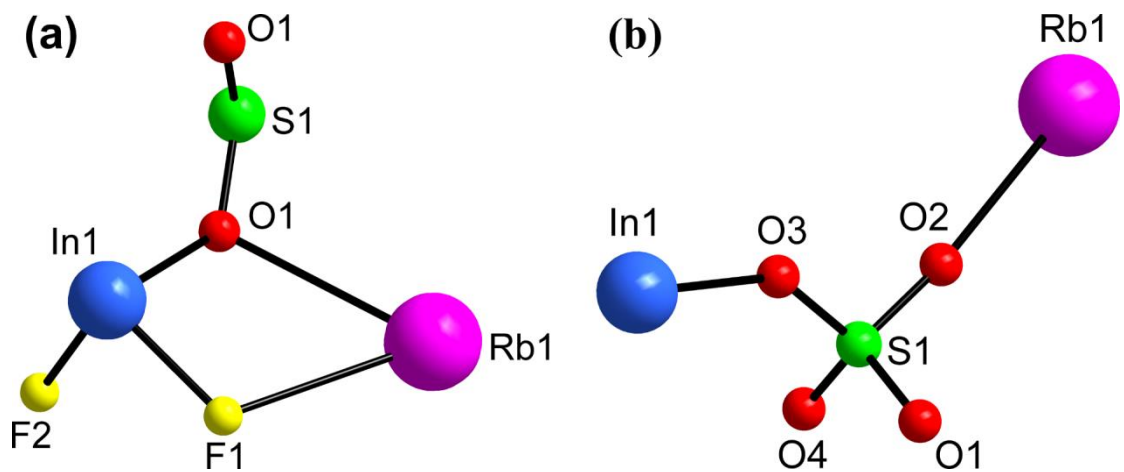


Figure S3. The asymmetric unit of (a) Rb₂InF₃(SO₄) and (b) Rb₃In(SO₄)₃.

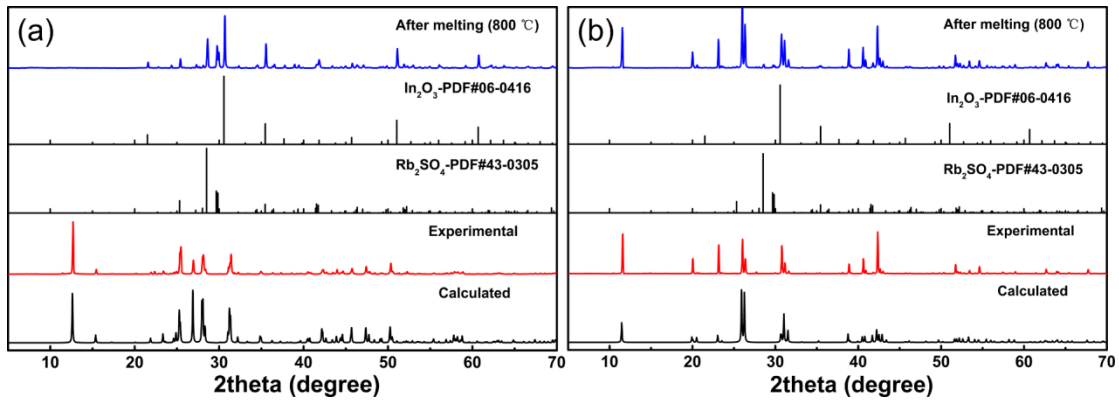


Figure S4. Powder X-ray diffraction patterns of (a) $\text{Rb}_2\text{InF}_3(\text{SO}_4)$ and (b) $\text{Rb}_3\text{In}(\text{SO}_4)_3$.

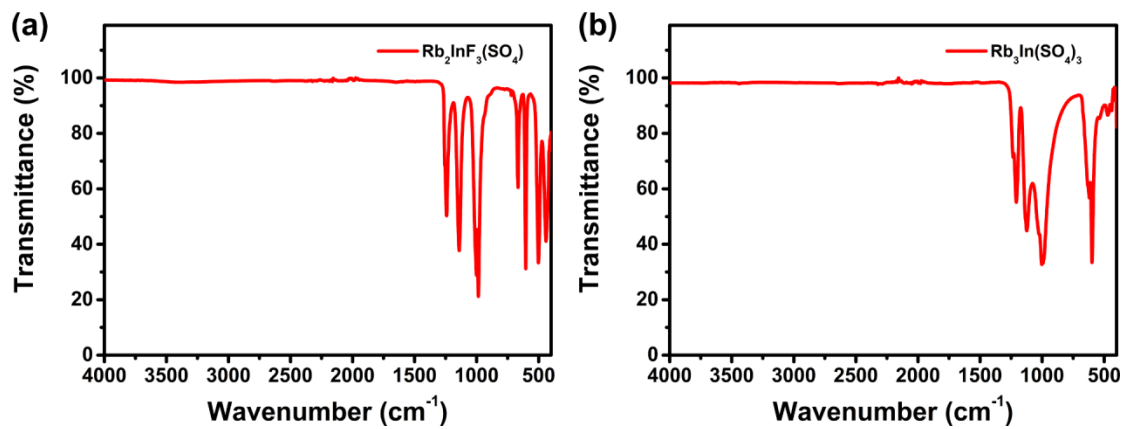


Figure S5. IR spectra of (a) $\text{Rb}_2\text{InF}_3(\text{SO}_4)$ and (b) $\text{Rb}_3\text{In}(\text{SO}_4)_3$.

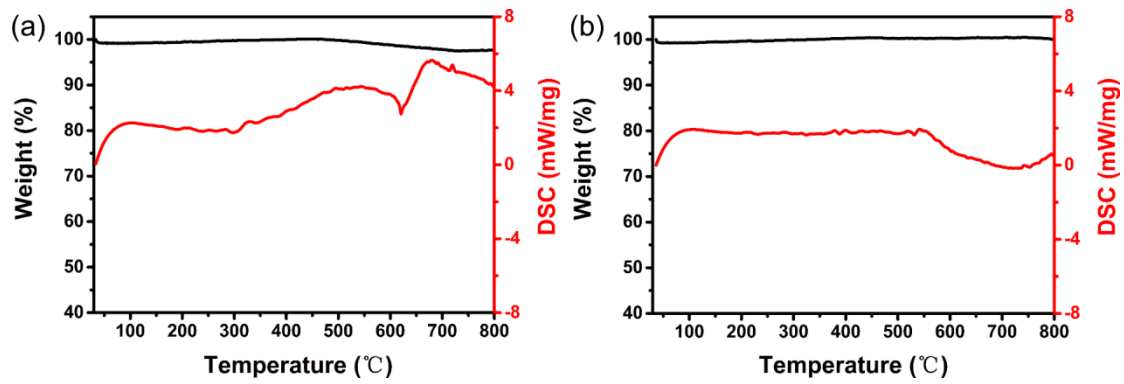


Figure S6. Thermogravimetric analyses of (a) $\text{Rb}_2\text{InF}_3(\text{SO}_4)$ and (b) $\text{Rb}_3\text{In}(\text{SO}_4)_3$ under a N_2 atmosphere.

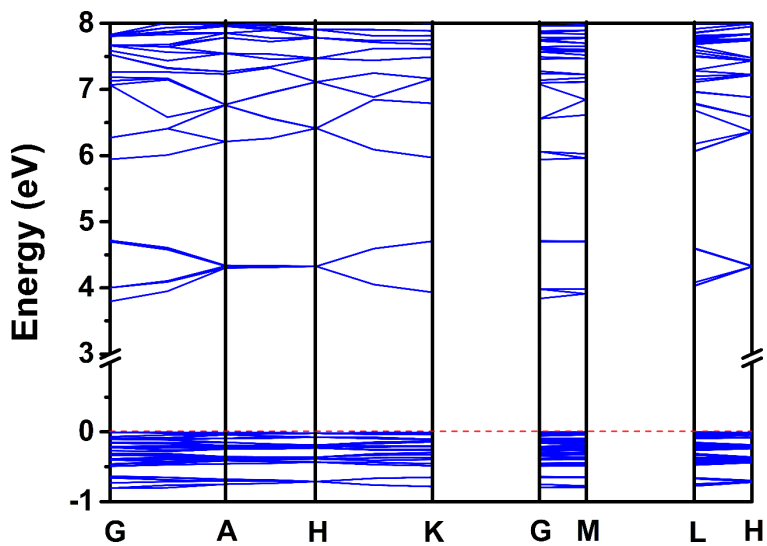


Figure S7. Calculated band structures of $\text{Rb}_3\text{In}(\text{SO}_4)_3$.

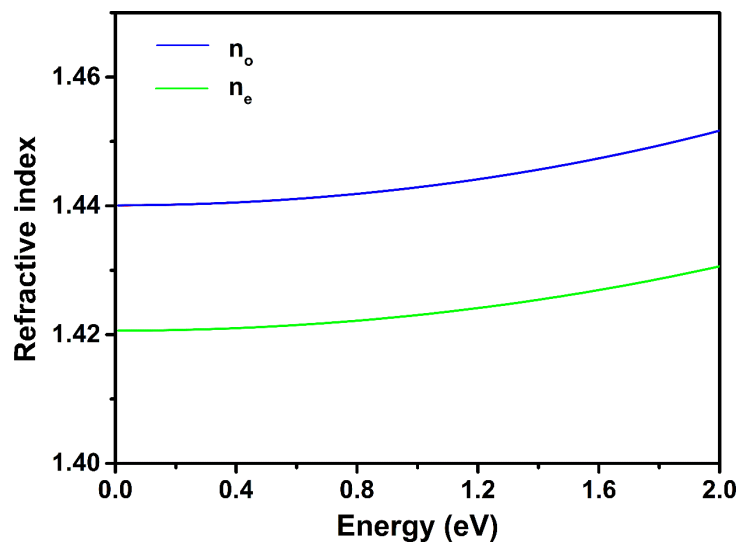


Figure S8. Calculated refractive indexes of $\text{Rb}_3\text{In}(\text{SO}_4)_3$.

References

1. S. J. Clark, M. D. Segall, C. J. Pickard, P. J. Hasnip, M. J. Probert, K. Refson and M. C. Payne, *Z. Kristallogr.*, 2005, **220**, 567-570.
2. W. Kohn and L. J. Sham, *Phys. Rev.*, 1965, **140**, 1133-1138.
3. J. P. Perdew, K. Burke and M. Ernzerhof, *Phys. Rev. Lett.*, 1996, **77**, 3865-3868.
4. L. Kleinman and D. M. Bylander, *Phys. Rev. Lett.*, 1982, **48**, 1425-1428.
5. H. J. Monkhorst and J. D. Pack, *Phys. Rev. B*, 1976, **13**, 5188-5192.
6. R. W. Godby, M. Schluter and L. J. Sham, *Phys. Rev. B*, 1988, **37**, 10159-10175.
7. E. D. Palik, *Handbook of Optical Constants of Solid*, Academic: New York, 1985.
8. J. Lin, M. H. Lee, Z. P. Liu, C. T. Chen and C. Pickard, *J. Phys. Rev. B*, 1999, **60**, 13380-13389.
9. Z. S. Lin, X. X. Jiang, L. Kang, P. F. Gong, S. Y. Luo and M. H. Lee, *J. Phys. D: Appl. Phys.*, 2014, **47**, 253001(253001)-253001(253019).
10. M. H. Lee, C. H. Yang and J. H. Jan, *Phys. Rev. B*, 2004, **70**, 235110-235120.